Design and Implementation of a Transduction System for the Measurement of a Weakly Nonlinear Mechanical Oscillator Project (Ultrasound sensor)

ME310 Instrumentation

April 4 - 25th, 2025

Section A1/A2: Farny & Walsh

Group 5:

Kantika Klomjoho

Xiangyi Han

Ariam Habtemariam

OBJECTIVE

The goal of this project is to experimentally determine the frequency response of a spring-mass-damper system. To achieve this, we developed a custom transduction setup to digitally measure the oscillation amplitude of the top mass under a range of driving frequencies. This project will require designing a measurement system that accurately collects data using a sensor and processes it to improve the quality and reliability of the output. By integrating principles of instrumentation and signal processing concepts as it applies to second-order mechanical systems, we will extract key parameters such as the natural frequency, damping ratio and peak amplitude. These parameters will then be used to characterize the behavior of the system.

THEORY

This experiment explores the behavior of a mechanical second-order system composed of two vertically aligned masses connected by a spring (Figure 1). The lower mass, m_b, is driven vertically by a motor and scotch yoke mechanism that produces sinusoidal motion at a variable frequency. The upper mass, m, responds dynamically through the spring and damping forces acting between the two masses.

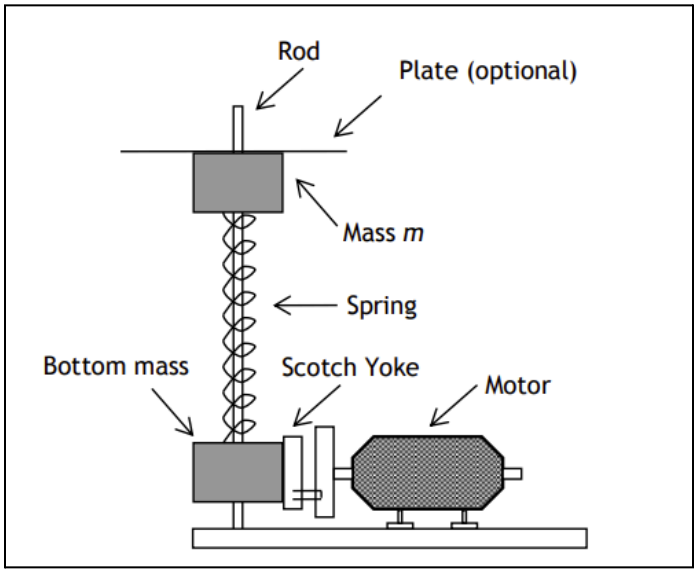

Figure 1: Diagram of the mechanical second order system.

At low driving frequencies, the spring has enough time to transfer force smoothly, and both masses move nearly together. As the driving frequency increases, the inertia of the upper

mass limits its ability to follow the lower mass's motion. This results in a growing difference between their displacements and introduces a frequency-dependent behavior characteristic of second-order systems. The upper mass experiences two main forces: a spring force that depends on its motion relative to the lower mass, and a damping force that resists motion and dissipates energy (Figure 2). Together, these forces define how the system responds to the sinusoidal input. At certain frequencies, the input energy is transferred efficiently, leading to resonance, where the amplitude of the upper mass's motion reaches a peak. Beyond resonance, the amplitude decreases, and the top mass lags further behind the bottom mass in phase.

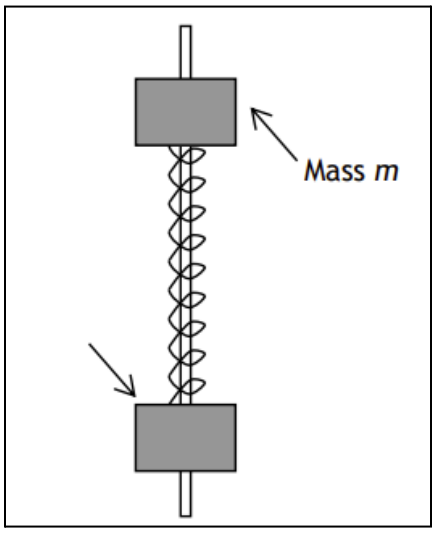

Figure 2: Diagram of the coupled masses arranged to slide on a rod.

These relationships are well captured in the theoretical behavior of second-order systems. For an underdamped system, the amplitude response increases with frequency up to resonance, then falls off as frequency continues to rise (Figure 3).

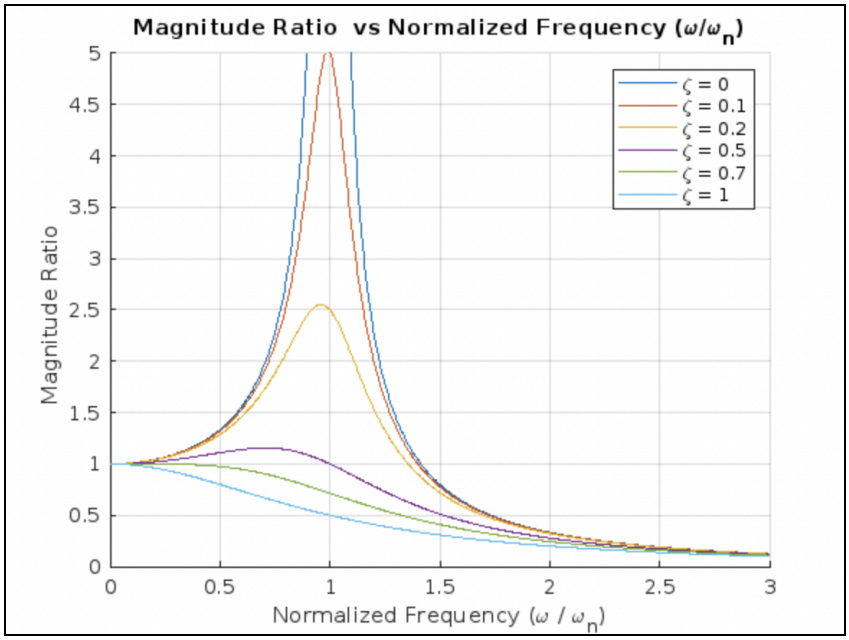

Figure 3: The magnitude ratio vs. normalized frequency graph.

At the same time, the phase of the upper mass's motion gradually shifts — from nearly in-phase at low frequencies, to approximately 90 degrees out of phase at resonance, and approaching 180 degrees out of phase at high frequencies (Figure 4). This combination of amplitude and phase behavior defines the full frequency response of the system.

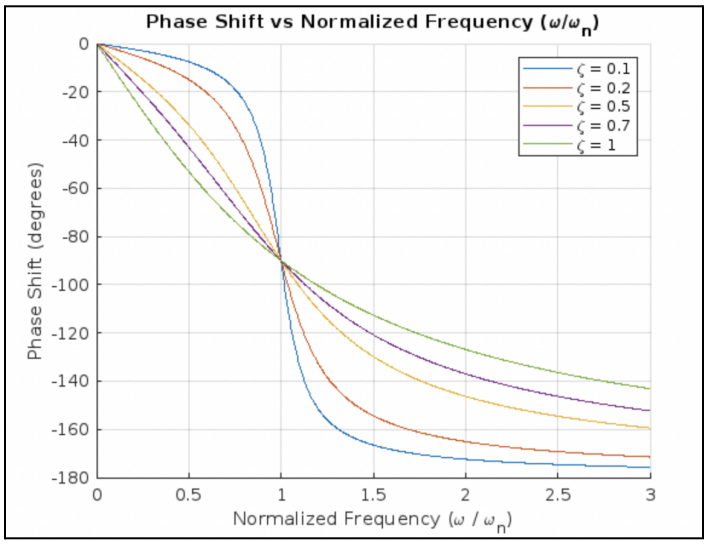

Figure 4: The phase shift vs. normalized frequency graph.

To track the motion of the upper mass, we implemented a non-contact ultrasonic transduction system. The sensor emits acoustic pulses toward the mass and measures the time-of-flight of the reflected echo. By calculating the delay between each transmitted pulse and

its corresponding echo, we obtain a real-time measurement of the top mass's position. This method allows for accurate and repeatable displacement tracking without physically contacting the system, which is especially valuable for high-speed or lightly damped oscillatory systems like this one. Although the system is modeled using linear equations, real-world conditions introduce small nonlinearities. These can arise from mechanical friction, misalignment, or imperfections in the spring or mounting. While these nonlinearities can lead to slight deviations from theoretical predictions, they are minor in this case and do not prevent the use of the linear model as a valid approximation for analyzing the system's frequency response.

EQUATION SUMMARY

The behavior of the mechanical oscillator is modeled as a damped, driven second-order system. To describe the motion of the upper mass under external forcing, we begin with the second-order differential equation that governs a mass-spring-damper system subjected to a sinusoidal base input. The equation below accounts for mass inertia, damping resistance, and spring restoring force:

$$m\ddot{x}(t) + c\dot{x}(t) + kx(t) = kx_b(t) \qquad (1)$$

where:

- x(t): displacement of the upper mass
- $x_b(t)$: displacement of the lower (driven) mass
- m: mass of the upper component (kg)
- c: damping coefficient (N*s/m)
- k: spring constant (N/m)
- $\dot{x}(t)$: velocity of the upper mass
- $\ddot{x}(t)$: acceleration of the upper mass

The system's natural frequency ω_n (rad/s) describes how fast it oscillates when released with no damping or forcing:

$$\omega_n = \sqrt{k/m} \qquad (2)$$

where

- k=spring constant (N/m)

- m = mass of system

The damping ratio ζ, a dimensionless parameter, indicates how oscillations decay over time and can be calculated by comparing the damping coefficient to its critical value:

$$\zeta = c/2\sqrt{km} \qquad (3)$$

where:

- *c*: damping coefficient (N*s/m)

For an underdamped system, the system oscillates at a damped natural frequency ω_d (rad/s) that is slightly lower than the natural frequency:

$$\omega_d = \omega_n\sqrt{1 - \zeta^2} \qquad (4)$$

To describe the sinusoidal behavior of the system, the input displacement from the motor (lower mass) is modeled as:

$$x(t) = Asin(\omega t) \qquad (5)$$

where:

- A: amplitude of the input motion (m)
- ω: driving angular frequency (rad.s)
- *t*: time (s)

The steady-state response of the upper mass is also sinusoidal but includes a gain and phase shift:

$$y(t) = A * M(\omega) * sin(\omega t + \phi(\omega)) \qquad (6)$$

where:

- y(t): displacement of the upper mass (m)
- M(ω): amplitude ratio (unitless)
- ϕ(ω): phase lag between input and output (radians)

The amplitude ratio quantifies how the output amplitude compares to the input amplitude at a given driving frequency:

$$M(\omega) = \frac{X(\omega)}{X_b(\omega)} \qquad (7)$$

where:

- X(ω): output amplitude of the upper mass (m)
- $X_b(\omega)$: input amplitude of the lower mass (m)

The phase shift describes how much the output motion (upper mass) lags behind the input (lower mass) as a function of driving frequency. This phase lag increases with frequency and provides insight into how the system transitions through resonance:

$$\phi(\omega) = -\tan^{-1}\left(\frac{2\zeta\omega/\omega_n}{1-(\omega/\omega_n)^2}\right) \qquad (8)$$

To measure displacement experimentally, the system uses ultrasonic time-of-flight sensing. The distance between the sensor and the top plate is calculated by:

$$x(t) = \frac{c*\Delta t}{2} \qquad (9)$$

where:

- c: speed of sound in air (m/s)
- Δt: round-trip time delay between pulse emission and echo reception (s)

Envelope form of the response for step input

$$y_{env}(t) = y_\infty - (y_0 - y_\infty)e^{-\xi\omega_n t} \qquad (10)$$

EQUIPMENT LIST

The following equipment was used to design, implement, and analyze the transduction system for the spring-mass-damper oscillator experiment.

Equipment	Manufacturer	Model number	Resolution
Motor controller	Minarik Drives	MM23211C	1 knob turn
DC Gearmotor	BISON Gear and engineering corp	011-190-0010	-N/A
Oscilloscope	BK Precision	2190E	1 Hz
Power supply	Agilent	E3631A	0.01V
Circuit board	AIRMAR	T1 development board	-N/A
A/D Breakout box	National Instrument	BNC-2090	-N/A
Caliper	TACKLIFE	DC01	0.0001m
Ultrasound Transducer	AIRMAR	AT-200	-N/A
Stroboscope	Sper Scientific	840009	-1rpm

Table 1: Our equipment used, along with the manufacturer, model number, and resolution where applicable.

Additional equipment and materials:

- Computer with MATLAB
- BNC cables
- Oscillator (two masses on a rod joined by a spring)
- Reflecting plate
- Banana plug to test hook clips
- Standard masses
- Ruler

METHODS AND MATERIALS

For this project, we used an ultrasonic sensor system to measure distance based on the time of flight; we created a set up where a pulse is emitted and its reflection is detected by a transducer. To set up the equipment, we wired the ultrasonic sensor module by connecting the J4 ground and 15V terminals to a DC power supply. To adjust the power supply, we selected +25V and used the adjustment knob to reduce the output to a steady 15V as suggested on the dev board data sheet. Following this, the transducer was securely attached to the J5 port, with downward-facing orientation towards the top plate, a component with a reflective surface of sufficient area to ensure reliable signal reflection. We then connected Channel 1 of the oscilloscope to the J6 port of the ultrasound sensor to monitor the sensor's output and verify the signal quality. The J1 port was connected with a jumper to configure the pulse repetition rate to 25 Hz, following the recommendations specified in the development board's datasheet for the AT200 transducer. Additionally, the pulse width was adjusted using the POT1 potentiometer on the development board to 320 milliseconds to ensure enough energy was transmitted in each ultrasonic pulse. The setup ensured consistent alignment and reliable echo detection, and our wiring diagram can be seen in Figure 5.

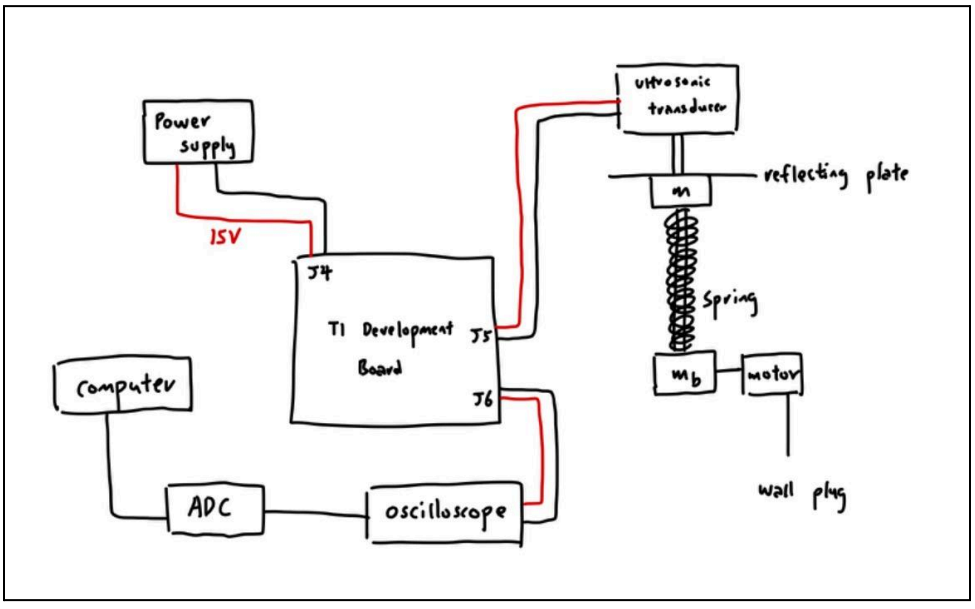

Figure 5: Wiring diagram for our system setup.

Then, we came up with a procedure to determine the spring constant of our oscillator. We incrementally added known masses to our plate, then measured and recorded the resulting vertical displacement to find the deflection. To determine the rotational speed (RPM) of the oscillator, we marked the spinning wheel and used a strobe light to visually match the wheel's motion to the flashing frequency. When the mark appeared stationary under the strobe, we recorded the corresponding frequency as the system's rotational speed. With the physical set up and baseline system parameters determined, we proceeded with data acquisition.

To acquire data, a custom MATLAB script was employed to interface with the Data Acquisition (DAQ) device. This script was configured to retrieve raw analog voltage data specifically from the channel connected to the output of our ultrasonic sensor. The DAQ's input configuration for this channel was set to SingleEnded, with a voltage measurement range of +/- 1 Volt. For each experimental trial, we established a high sampling rate of 250,000 samples per second (250 kHz) and recorded data for a duration of 5 seconds. This elevated sampling rate was chosen to ensure the precise capture of the rapid voltage fluctuations characteristic of ultrasonic echo pulses. We observed that increasing the sampling rate to this value resulted in a smoother and more continuous representation of our processed distance-versus-time data. This consistent sampling frequency of 250 kHz (the maximum rate supported by our DAQ) was maintained throughout the entire experiment. This decision was made by the fact that the ultrasonic signals of interest operate within the 200 kHz frequency range. We opted to utilize the maximum available sampling frequency from the DAQ, acknowledging that even this rate might be theoretically optimal considering the 200 kHz operating frequency of our ultrasonic sensor. Employing a lower sampling rate could have resulted in insufficient Nyquist frequency, potentially leading to aliasing, distorting the recorded signal and compromising the accuracy of our subsequent analysis. We decided to record for 5 seconds per trial to allow for enough time to collect a sufficient amount of data–a 5-second window ensured multiple oscillations could be seen in each trial. This allowed for more complete graphs of the system's motion, making it easier to visualize and analyze periodic trends. We conducted 25 trials total from both the increasing sweep and decreasing sweep.

DATA

In addition to capturing the ultrasound pulse data as voltage signals from the oscilloscope using MATLAB—which will be discussed in detail in the Analysis section—raw data were collected to determine the spring constant of the system. Table 2 presents the measured displacements of the spring corresponding to various applied masses.

Top Plate Mass (g)		132.2
Top Collar Mass (g)		138.9
Mass Added (kg)	Total Mass (kg)	Distance between Sensor and Top mass (m)
0.15	0.421	0.01
0.20	0.471	0.015
0.30	0.571	0.02
0.40	0.671	0.035
0.70	0.971	0.05
1.2	1.471	0.105

Table 2: Mass and Displacement of spring in the Mechanical Oscillator System

ANALYSIS

1. Spring Constant (k)

To determine the spring constant k, known masses were incrementally added to the upper plate, and the corresponding displacement—measured as the distance by which the spring compressed relative to the sensor—was recorded. By applying Hooke's Law ($F=kx$), a linear relationship between the applied force (F) and the resulting displacement (x) was established. The spring constant k was then calculated as the slope of the force versus displacement graph.

This value plays a key role in characterizing the system, influencing how it responds to input and governing the dynamic behavior of the oscillator.

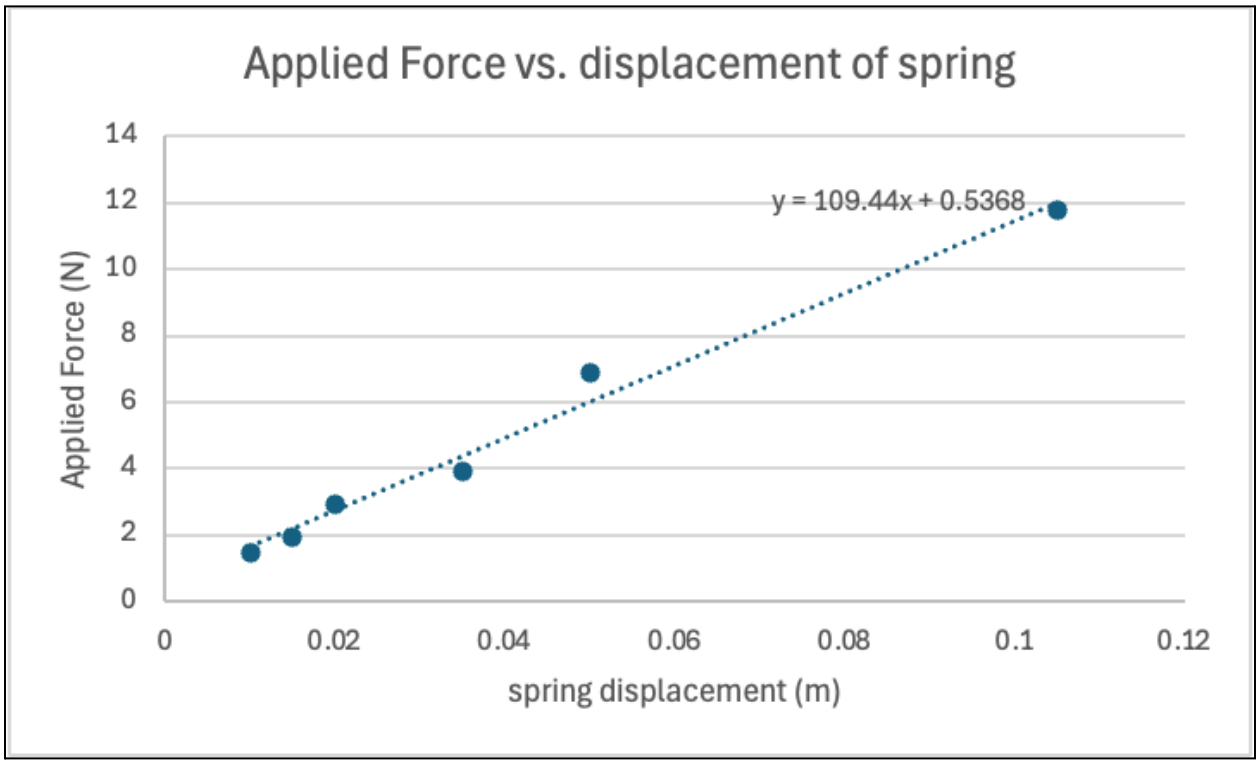

Figure 6: Applied force vs. displacement of upper mass.

$$The\ slope\ of\ the\ force\ versus\ displacement\ graph\ was\ calculated\ to\ be\ 109\ N/m$$

$$Thus,\ k\ =\ 109.44\ N/m$$

2. Natural Frequency (ω_n) and Damping Ratio (ξ)

Two approaches were employed to determine the natural frequency of the system: a theoretical calculation and an experimental calculation from the measurement. In the theoretical approach, ω_n was calculated using previously determined spring constant k and combined mass of top plate with top collar based on Equation 2 as shown below

$$\omega_{n,theoretical} = \sqrt{\frac{k}{m}} = \sqrt{\frac{109.44\ \frac{kg\ m}{s^2}}{0.271\ kg}} = 20.10\ rad/s$$

The system was allowed to oscillate freely without any external driving frequency, meaning that the observed oscillation occurred at its damped natural frequency, with amplitude decay governed by the damping ratio ξ and ω_n. The time intervals between each emitted ultrasound pulse and its corresponding echo were measured, and these values were converted

into distance using the speed of sound in air, accounting for the round-trip travel time. This process yielded a time series of displacement data for the top mass. The detailed explanation of the code functions and data extraction procedures is provided in the following section.

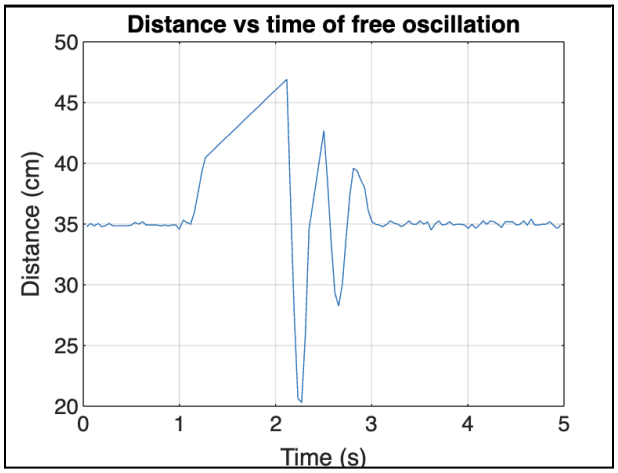

Figure 7: The distance of the top plate vs time plot for the free oscillation

The resulting displacement-time plot exhibited a decaying oscillatory pattern, indicating that the system is underdamped and responding to a step-like input force (from initially compressing and releasing the spring). To analyze this behavior, the envelope of the response—characteristic of a second-order underdamped system—was used to determine the slope of the decay, using Equation 10.

$$y_{env}(t) = y_{\infty} - (y_0 - y_{\infty})e^{-\xi\omega_n t}$$

The envelope of the decaying oscillation was linearized by taking the natural logarithm of the normalized displacement response. The equation used is:

$$ln(\frac{y_{env}(t)-y_{\infty}}{y_0-y_{\infty}}) = -\xi\omega_n t$$

Here, $y_{env}(t)$ represents the displacement of the top mass at time t. y_0 is the initial displacement before the step input, and y_{∞} is the final steady-state displacement. This linear relationship allows the slope of the plot of $ln(\frac{y_{env}(t)-y_{\infty}}{y_0-y_{\infty}})$ and time returned the slope of the decay as $-\xi\omega_n$ where ξ is the damping ratio and ω_n is the natural frequency.

To generate the envelope data and the corresponding plot, the ginput function in MATLAB was used to manually select the peak values of the decaying oscillation along with

their corresponding times (see appendix B). The slope of the decay was determined to be -1.3216 rad/s. Thus, we have

$$\xi\omega_n = 1.3216\, rad/s$$

To determine ξ, the damped natural frequency ωd was extracted from the time between successive peaks (the period T_d) using the following relationship:$\omega_d = \frac{2\pi}{T_d}\ (rad/s)$.

MATLAB returned :

$$\omega_d = 17.22\, rad/s$$

The period T_d was calculated from the average of the measured peak intervals using MATLAB (see appendix A). Recall the relationship between the natural frequency ω_n, damping ratio ξ and damped natural frequency ω_d from Equation 4:

$$\omega_d = \omega_n\sqrt{1 - \xi^2},$$

By substituting ω_d and $\xi\omega_n$ determined previously into the above relationship, we can solve for both ξ and ω_n. The MATLAb script used for this calculation was presented in Appendix A.

$$\omega_{n,\,experimental} = 17.27\, rad/s$$

$$\xi = 0.076$$

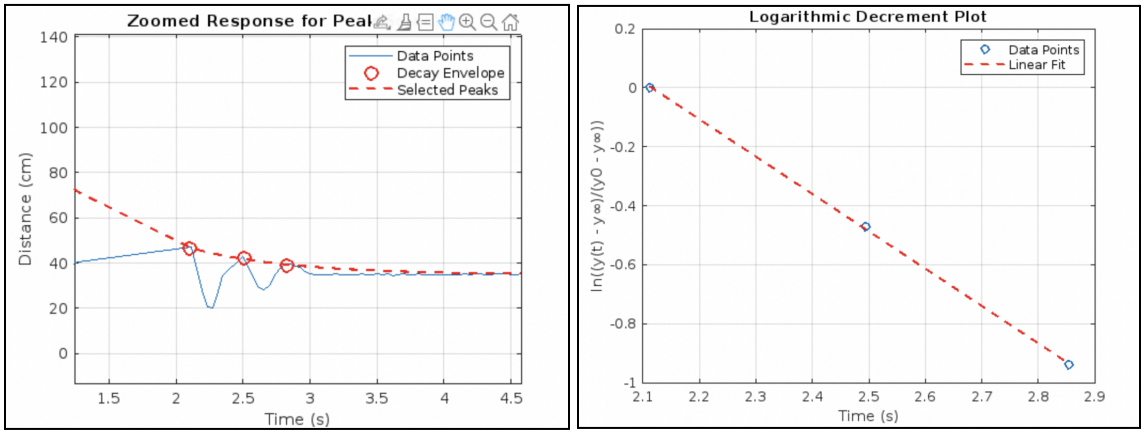

Figure 8: The decaying envelope slope along with the linearized logarithmic decrement plot.

The calculated damping ratio ξ is found to be less than 1, confirming that the system behaves as a lightly damped second-order oscillator. This is consistent with the oscillatory response observed during free vibration, where the system exhibits decaying sinusoidal motion as energy is gradually dissipated due to damping. Since the damping ratio ξ is less than 1, the system is capable of exhibiting resonance. This means that when subjected to input near its natural frequency, the system can experience amplified oscillations. The resonance behavior of the system will be determined and discussed in the following section. As for the calculated ω_n and ω_d , due to the fact that the system is underdamped, ω_d is slightly lower than ω_n, as energy is lost over time due to damping.

3. Damping coefficients c

The damping coefficient c is a parameter that characterizes the energy dissipation in the mass-spring system and plays a crucial role in determining its dynamic response to the sinusoidal driving force from the scotch yoke mechanism. It influences how the amplitude of the top mass's oscillation varies with the driving frequency and the phase relationship between the input and output motions. Damping coefficients c and critical damping coefficients can be calculated with the equation :

$$c = 2\xi\sqrt{km} = 2\xi m\omega_n = 2(0.076)(0.271)(17.27) = 0.711\ N{\cdot}s/m$$

$$c_c = 2\sqrt{km} = 2m\omega_n = 2(0.271)(17.27) = 9.36\ N{\cdot}s/m$$

4. Amplitude as a function of time of the top mass x(t)

The MATLAB script detailed in Appendix B processes raw ultrasonic sensor data, represented as voltage over time, to extract the distance to the top mass (x(t)) as a function of time for various driving frequencies. Data processing relies on identifying transmitted ultrasonic pulses and their echoes. The script begins by loading the time and signal data, then estimates the sampling rate by determining the average time difference between consecutive data points and taking its inverse. As noted, this calculated sampling rate was confirmed to match the 250 kHz sampling rate used during data acquisition via the DAQ board. For an initial assessment, the raw

voltage signal of pulse and echo is plotted against time. To isolate the relevant ultrasonic frequency range (around 200 kHz) and eliminate any background noise, a bandpass Butterworth filter is applied. The cutoff frequencies for this filter were determined by analyzing the dominant frequency of the raw ultrasonic pulses using the FFT function in MATLAB.

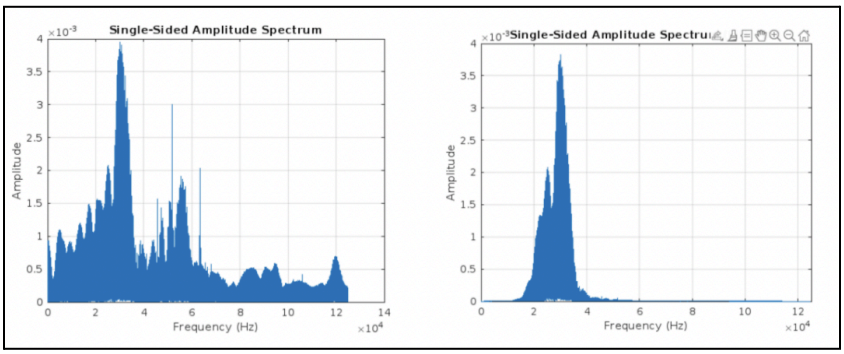

Figure 9: The raw signal frequency before and after applying the bandpass filter.

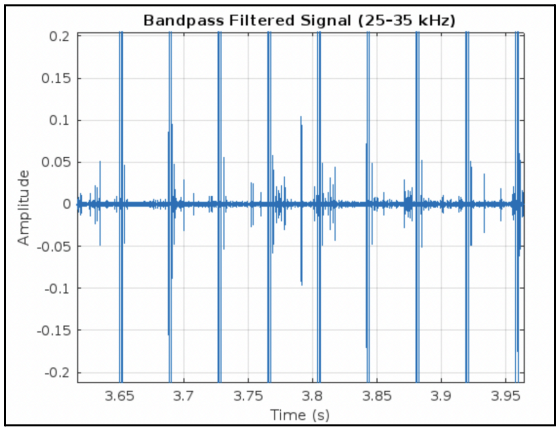

Figure 10: A zoomed-in view of the raw signal after filtering, with visible detected pulses and their corresponding echoes.

The script operates based on the detected pulses and their corresponding echoes in the filtered signal. A pulse is identified when the sensor signal exceeds a defined amplitude threshold of 2V. The echo is then located by scanning forward for a subsequent threshold crossing at 0.23V. These threshold values were estimated by analyzing the raw voltage data. The search for an echo begins after a duration determined by the sensor's pulse width, which was set to 320 microseconds to avoid immediate re-triggering. To prevent misidentification of echoes, the search is confined to a window based on half the expected pulse repetition rate. The code then searches for the next pulse based on the pulse rate of 25 Hz (or 0.004 seconds) and repeats

the process in a loop. For each detected pulse-echo pair, the time difference between their occurrences is calculated. This time difference is then used to compute the distance to the reflecting plate on the upper mass using the speed of sound in air at 25℃ (c = 343 m/s), accounting for the round trip by dividing the total travel time by two. The resulting distances are converted to centimeters. These calculated distances are then plotted against the time instances of the corresponding pulse emissions. Selected sample plots were presented in the Results section figure 14.

A total of 25 distances Vs. time plots were generated at various knob settings, both incrementing and decrementing, to observe the system's response. The script also identified and extracted the amplitudes for each setting, and the results were compiled and presented in Table 4 in the result section.

5. Amplitude of the lower mass (Xb)

The amplitude of the lower mass is quantified as the input to the system and can be determined by the distance traveled by the bearing on the motor's shaft. The Scotch yoke mechanism facilitates vertical motion of the bottom mass, coordinating with the rotational motion of the motor. Given a measured diameter of 6.0 cm for the motor's shaft (peak-to-peak amplitude), the input amplitude of the system can be derived as half of this value, since the vertical motion is proportional to the radius of the motor's shaft.

$$X_b = \frac{6.0}{2} cm = 3.0\, cm$$

6. Driving Frequency

The driving frequency of the system's input corresponds to the dominant frequency present in the derived distance data, as obtained using the MATLAB script. To analyze this, the script first interpolates the distance data to create a uniformly sampled time series, enabling the application of a Fast Fourier Transform (FFT). The FFT reveals the dominant frequency component in the system's response. As seen in Figure 11 below, the sample FFT plot from the knob setting of 20 reveals 1.21 Hz as the dominant frequency.

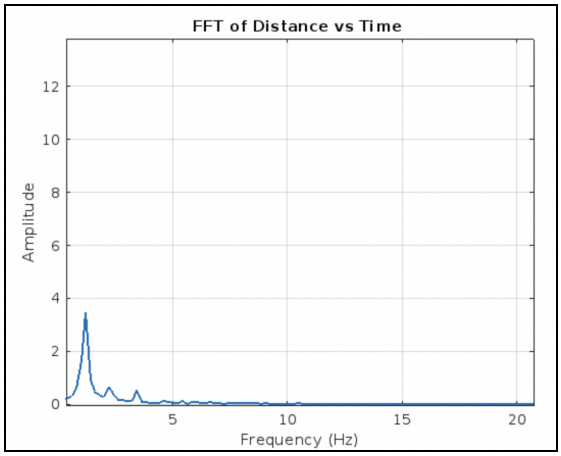

Figure 11: FFT plot from the knob setting of 20 revealing the dominant frequency as the system's driving frequency

The script also identified and extracted the dominant frequency for each knob setting, and the results were compiled and presented in Table 4. The driving frequency was controlled by the knob settings on the motor controller, with higher knob values corresponding to higher driving frequencies. This driving frequency directly influences the relative movement between the top and bottom masses and shapes how the system responds to the inputs; this topic will be discussed in more detail in the Frequency Response section.

To ensure the accuracy of the driving frequency determined, an independent measurement was conducted using a stroboscope. When the flash frequency of the stroboscope matches the rotational frequency of a marked point on the motor's output shaft, that point will appear to be stationary to the observer. By carefully adjusting the stroboscope's flash frequency until this freezing effect is observed, the driving frequency of the motor, and thus the input to the mechanical system, can be directly measured and compared with the value indicated by the motor controller.

The reading we obtained when the knob was set to 22 was 195 RPM. Converting this to radians per second gives:

195 RPM * [2π rad / 1 rotation]*[1 min / 60 sec] = 10.2 rad/s for a knob setting of 22.

This value agrees with the frequency obtained via the FFT method which was 10.739 rad/s for a knob setting of 22. with only slight variations. This minor discrepancy is likely attributable to the

limitations of our visual perception when judging the synchronization of the stroboscope's flashes with the moving component.

7. Frequency Response

To analyze the system's response to the sinusoidal input from the scotch yoke mechanism across different driving frequencies, the **magnitude ratio (M)** was determined. As established earlier, the system behaves as an underdamped second-order system subjected to sinusoidal forcing. The steady-state output response, y(t), can be generally described as:

$$x(t) = KAM(\omega)(sin(\omega t) + \phi) + KA_0 + O$$

Given the assumption of a sensor sensitivity (K) of 1 and no offset ($KA_0 + O = 0$), and focusing solely on the amplitude relationship, the magnitude of the output is proportional to the magnitude of the input scaled by the magnitude ratio:

$$x(t) = KAM(\omega)$$

Where A denotes the amplitude of the input, x(t) represents the amplitude of the output.

The magnitude ratio M was calculated for each driving frequency, for both increasing and decreasing frequency sweeps, and these values are presented in Table 4 in the Results section. To visualize the system's frequency response, M was then plotted against the driving frequency in Figure 12 in the Results section. The plot will also include theoretical M determined by the experimentally determined values for natural frequency and damping ratio.

As expected for an underdamped system, the frequency response plot exhibits resonance behavior, where the output amplitude is amplified (M>1) when the driving frequency is near the system's natural frequency. The plot shows a peak magnitude ratio of 2.256 at a corresponding driving frequency of 15.01 Hz. The sharpness of the resonance can also be determined with quality factor Q as follows

$$Q = M_{max} = 2.256$$

The input frequency corresponding to M_{max} is identified as the **system's resonance frequency**.

$$\omega_{r,\,experimental} = 15.01\,rad/s$$

This system resonance frequency can also be calculated theoretically using the previously determined damping ratio (ζ) and natural frequency (ω_n) via the following equation:

$$\omega_r = \omega_n\sqrt{1 - 2\xi^2}$$

$$\omega_{r,theoretical} = 17.27\sqrt{1 - 2(0.076)^2} = 17.17\,rad/s$$

The discrepancies between the resonance frequencies (ω_r) obtained using the two approaches will be addressed in the Uncertainty Analysis section.

Magnitude ratio can also be determined theoretically by plug in in system parameters and driving frequency into the equation :

$$M(\omega) = \frac{1}{\sqrt{(1-(\frac{\omega}{\omega_n})^2)^2+(2\zeta\frac{\omega}{\omega_n})^2}}$$

Example calculation for driving frequency of 12.1204 rad/s

$$M(12.1204)_{theoretical} = \frac{1}{\sqrt{(1-(\frac{12.1204}{17.27})^2)^2+(2(0.076)\frac{12.1204}{17.27})^2}} = 1.928$$

Figure 12 on the result section will show this theoretical M along with experimental values and discuss any discrepancies observed. From the system's resonance frequency, we can quantify its response across a range of driving frequencies. Specifically, the amplitude and the phase of the top mass's motion relative to the bottom mass varies with the input frequency. When the driving frequency is much lower than the resonance frequency, the top mass closely follows the bottom mass's motion, remaining nearly in phase, resulting in minimal relative displacement. At resonance, the relative displacement reaches its maximum, accompanied by a phase lag of approximately -90 degrees. Conversely, when the driving frequency exceeds the natural

frequency, the top mass begins to lag further behind the bottom mass, and the amplitude of relative motion decreases. This expected trend in dynamic behavior is consistent with the experimental data presented in Table 4.

8. Phase Shift (ϕ)

We observed the phase response between the two masses changing with the driving frequency as expected for a second-order system subjected to sinusoidal forcing. The equation for the phase shift (ϕ) of the output relative to the input for a second-order system with a sinusoidal input is given by: $\Phi(\omega)_{theoretical} = \ - \ tan^{-1}(\frac{2\xi\frac{\omega}{\omega_n}}{1-(\frac{\omega}{\omega_n})^2})$

Example calculation for driving frequency of 12.1204 rad/s

$$\Phi(12.1204)_{theoretical} = \ - \ tan^{-1}(\frac{2(0.076)\frac{12.1204}{17.27}}{1-(\frac{12.1204}{17.27})^2}) = \ - \ 0.2072 \, rad$$

By plugging in the damping ratio, natural frequency, and driving frequency data from Table X, we were able to determine the theoretical phase lag corresponding to each driving frequency. These calculated phase lag results are presented in Table X within the Results section. To visualize the system's dynamic relationship, the phase shift between the top mass's displacement (output) and the bottom mass's displacement (input) was plotted against the driving frequency, as shown in Figure 15 of the Results section. As anticipated for a second-order system, the phase relationship from figure 15 changes significantly with the driving frequency. When the driving frequency is much lower than the system's natural frequency, the phase of the output (top mass displacement) lags behind the input (bottom mass displacement) by a small amount, nearing 0 degrees (0 radians). As the driving frequency approaches the natural frequency, the phase lag increases, nearing -90 degrees (1.57 radians). At frequencies above the natural frequency, the phase lag continues to increase, asymptotically approaching -180 degrees (π radians), indicating that the output response becomes more out of phase with the input. Figure 15 in the result section shows this phase shift plot.

UNCERTAINTY ANALYSIS

1. **DAQ board**

The DAQ board specification sheet was provided for this project, and it contains all the necessary information to determine the measurement uncertainty of the equipment. Since our design uses an input range of [-1, 1], the effective range is 2 V. According to the DAQ board's specifications, the uncertainty may arise from several factors, including resolution, accuracy, and sensitivity.

$$U_{DAQ,resolution} = \pm \frac{V_{res}}{2}$$

where $V_{res} = \frac{V_{FS}}{2^n} = \frac{2V}{2^{16}} = 3.052\ X\ 10^{-5} V$

$$U_{DAQ,resolution} = 1.526\ x\ 10^{-5} V$$

$$U_{DAQ,accuracy} = Reading(GainError) + Range(OffsetError) + NoiseUncertainty$$

$U_{DAQ,accuracy} = 360\mu V$ (given)

$U_{DAQ,sensitivity} = 12\mu V$ (given)

$$U_{DAQ} = \sqrt{(3.052\ x\ 10^{-5} V)^2 + (360x10^{-6} V)^2 + (12\ x\ 10^{-6} V)^2}$$

$=3.615 \text{ x } 10^{-4}\ V$

2. k, the spring constant

The spring constant k was determined using Hooke's Law, F = kx, where F is the force applied by different masses and x is the corresponding displacement of the upper plate. The displacement was measured using a yardstick, while the force was calculated from the known masses and gravitational acceleration. To account for the uncertainty of k, we will need to account for both the random and systematic uncertainties of k. To calculate the random uncertainty of k, we will need to find the k value per trial, which is shown in Table 3 below and then find the scatter uncertainty of all the k values using the formula:

$$U_{P,x} = t_v 95\% \frac{S_x}{\sqrt{N}}$$

where t_v = student t-value

S_x = standard deviation

v = N-1

Table 3

Δ F (N)	Δ x (m)	k (N/m)
0.4905	0.005	98.1
0.981	0.005	196.2
0.981	0.015	65.4
2.943	0.015	196.2
4.905	0.05	98.1

Table 3: k slope values from the six added masses to the second-order system

$U_{P,k}$, random uncertainty for k

$U_{P,k} = t_v 95\% \frac{S_x}{\sqrt{N}}$ where $S_x = \sqrt{\frac{\Sigma(S_i - \overline{S})^2}{N-1}}$

$\overline{k} = \frac{98.1+196.2+65.4+196.2+98.1}{5} = 130.8 N/m$

$S_x = \sqrt{\frac{\Sigma(S_i - \overline{S})^2}{N-1}} = \sqrt{\frac{14970.06}{4}} = 61.18 N/m$

$U_{P,k} = (2.770)(\frac{61.176}{\sqrt{5}}) = 75.78 N/m$ (95%)

The systematic uncertainty in the displacement arises from the resolution limit of the yardstick, which has a smallest division of 0.125 inches. Since labeled masses were used, the systematic uncertainty in the applied force is assumed to be negligible. The systematic uncertainty for the displacement can be calculated using the formula:

$$U_{B,resolution,x} = \pm \frac{resolution}{2}$$

$U_{B,resolution,\Delta x} = \pm \frac{0.125 inches}{2} = 0.0625 inches [\frac{0.0254m}{1\ inch}] = 0.001588m$

$U_{B,k} = \frac{\delta f}{\delta \Delta x} U_{B,\Delta x} = \left| \frac{\overline{F}}{\overline{\Delta x}^2} \right|$ (0.001588m)

$$U_{B,k} = \left|\frac{4.823N}{(0.039m)^2}\right|(0.0016m) = 4.990N/m$$

$$U_k = \sqrt{U_{P,k}^{\ 2} + U_{B,k}^{\ 2}} = \sqrt{(75.78N/m)^2 + (4.990N/m)^2} = 75.95N/m$$

k = 109.4N/m $\pm$ 75.95 N/m

3. ω_n , the natural frequency (theoretical)

The ω_n is determined from the spring constant k and mass m. Since m is assumed to have a negligible uncertainty, the uncertainty of the natural frequency will only depend on k. To calculate the uncertainty, we would need to use error propagation.

$$\omega_{n,theoretical} = \sqrt{\frac{k}{m}} = \sqrt{\frac{109\ \frac{kg\,m}{s^2}}{0.271\ kg}} = 20.06\ rad/s$$

$$U_{\omega_n} = \sqrt{\left(\frac{\delta\omega}{dk}U_k\right)^2 + \left(\frac{\delta\omega}{dm}U_m\right)^2}$$

$$= \sqrt{\left[\left(\frac{1}{2m\sqrt{\frac{k}{m}}}\right)(75.95N/m)\right]^2 + \left[\left(-\frac{k}{2\sqrt{\frac{k}{m}}m^2}\right)(0)\right]^2}$$

$$= \sqrt{(0.092s/kg * 75.95N/m)^2 + (0)^2} = 7.808\ rad/s$$

$\omega_n = 20.06\ rad/s \pm 7.808\ rad/s$

4. ξ , the damping ratio.

The damping ratio in this design project is determined from the free oscillation response of a second-order system. The envelope of the system's response can be described using the equation:

$$y_{env}(t) = y_\infty + \Delta e^{-\xi\omega_n t} \ or\ y_{env}(t) = y_\infty + \Delta e^{-t/\tau}$$

where τ is the time constant, ξ is the damping ratio, and ω_n is the natural frequency. To calculate the uncertainty of the damping ratio, the parameters on which it depends are first identified. From the relationships:

$$\tau = \frac{1}{\xi\omega_n} \text{ and } \omega_n = \frac{\omega_d}{\sqrt{1-\xi^2}}, \text{ where } \omega_d = \frac{2\pi}{T_d}$$

We can conclude that τ is a function of both the damping ratio and the damper period. Therefore, we can invert this relationship to express the damping ratio as a function of the time constant τ and the damped period T_d. The relationship for ξ with respect to the time constant and damped period is:

$$\xi = \frac{\tau}{\sqrt{\tau^2+(\frac{T_d}{2\pi})^2}}$$

The damped period T_d is the time between each peak of the oscillation, and the time constant is the negative reciprocal of the slope from the natural log of the free oscillation graph. Since there were only three available peaks from figure 8 it resulted in two different T_d and τ. This meant that the student t value for this uncertainty would be very big since the data is not scattered enough. In addition, since the oscillation graph is extracted from the DAQ board and then to MATLAB, the uncertainty for both T_d and τ would also include uncertainties from the DAQ board. Given from the spec sheet, the time resolution for the DAQ board is 50ns. Using those, we can then calculate the uncertainty of the damping ratio.

First, to find the damped period uncertainty:

$$\overline{T_d} = \frac{0.38502+0.30801}{2} = 0.3465s$$

$$S_x = \sqrt{\frac{\Sigma(S_i-\bar{S})^2}{N-1}} = \sqrt{0.002965} = 0.05445s$$

$$U_{P,T_d} = (12.706)(\frac{0.05445}{\sqrt{2}}) = 0.4892s \ (95\%)$$

$$U_{T_d} = \sqrt{(0.4892s)^2 + (50ns)^2} = 0.4892s$$

Next to find the time constant uncertainty:

$$\bar{\tau} = \frac{0.8991+0.6317}{2} = 0.7654s$$

$$S_x = \sqrt{\frac{\Sigma(S_i - \bar{S})^2}{N-1}} = \sqrt{0.03575} = 0.1891s$$

$$U_{P,\tau} = (12.706)(\frac{0.1891}{\sqrt{2}}) = 1.699s \text{ (95\%)}$$

$$U_\tau = \sqrt{(1.699s)^2 + (50ns)^2} = 1.699s$$

Now for the damping ratio uncertainty:

$$\xi = \frac{\tau}{\sqrt{\tau^2 + (\frac{T_d}{2\pi})^2}}$$

$$U_\xi = \sqrt{(\frac{\delta\xi}{d\tau}U_\tau)^2 + (\frac{\delta\xi}{dT_d}U_{T_d})^2}$$

$$U_\xi = \sqrt{[0.053(1.699)]^2 + [-0.041(0.4892)]^2}$$

$$= 0.09$$

$$\xi = 0.076 \pm 0.09$$

5. ω_n , the natural frequency (experimental)

Compared to the theoretical natural frequency, which was calculated from the equation:

$$\omega_{n,theoretical} = \sqrt{\frac{k}{m}}$$

The experimental natural frequency was calculated by plugging in the values of ω_d and $\xi\omega_n$ determined using the free oscillation into the equation:

$$\omega_n = \frac{\omega_d}{\sqrt{1-\xi^2}} = \frac{2\pi}{T_d\sqrt{1-\xi^2}}$$

This means that the experimental natural frequency is based on the uncertainty of the damping frequency and the damping ratio.

$$\omega_n = \frac{17.22 rad/s}{\sqrt{1-(0.076)^2}} = 17.27 rad/s$$

$$U_{\omega_n} = \sqrt{\left(\frac{\delta\omega_n}{d\xi} U_\xi\right)^2 + \left(\frac{\delta\omega_n}{d\omega_d} U_{\omega_d}\right)^2}$$

where $U_{\omega_d} = \frac{2\pi}{T_d^2} * U_{T_d}$

$$= \sqrt{(1.34 rad/s * 0.09)^2 + (8.9 rad/s * 1.003)^2} = 8.9 rad/s$$

$$\omega_n = 17.27 rad/s \pm 8.9 rad/s$$

6. ω_r , the resonance frequency (theoretical)

The resonance frequency is determined from the natural frequency ω_n and the damping ratio ξ. To calculate the uncertainty in for the resonance frequency, we will propagate the uncertainties of both the natural frequency and the damping ratio.

$$\omega_r = \omega_n \sqrt{1 - 2\xi^2}$$

$$U_{\omega_r} = \sqrt{\left(\frac{\delta\omega_r}{\delta\omega_n} U_{\omega_n}\right)^2 + \left(\frac{\delta\omega_r}{\delta\xi} U_\xi\right)^2}$$

$$= \sqrt{[(1 - 2\xi)^2 (U_{\omega_n})]^2 + \left(\frac{-2\omega_n \xi}{\sqrt{1-2\xi^2}} U_\xi\right)^2}$$

$$= \sqrt{[(0.994)(7.81)]^2 + [-2.61(0.09)]^2}$$

$$\omega_r = 17.17 rad/s \pm 7.7 rad/s$$

7. c , the damping coefficient

The damping coefficient is calculated using the damping ratio, spring constant and the mass. Therefore the uncertainty would need the uncertainty of all three parameters.

$c = 2\xi\sqrt{km}$ =0.711

$$U_c = \sqrt{\left(\frac{\delta c}{\delta \xi} U_\xi\right)^2 + \left(\frac{\delta c}{\delta k} U_k\right)^2 + (0)^2}$$

$$U_c = \sqrt{(9.36 * 0.09)^2 + (0.0065 * 75.95)^2 + (0)^2}$$

$$c = 0.711 \pm 0.89$$

8. M, the magnitude ratio (theoretical)

The magnitude ratio in the designed project is calculated from both the plotting of the amplitude peaks and theoretically from the natural frequency and the damping ratio. Theoretically, you can determine the magnitude ratio with the formula:

$$M(\omega) = \frac{1}{\sqrt{\left(1-\left(\frac{\omega}{\omega_n}\right)^2\right)^2 - \left(\frac{2\xi\omega}{\omega_n}\right)^2}}$$

Therefore, to determine the uncertainty for the magnitude ratio with respect to the parameters it depends on, it would be:

$$U_{M(\omega)} = \sqrt{\left(\frac{\delta M(\omega)}{\delta \xi} U_\xi\right)^2 + \left(\frac{\delta M(\omega)}{\delta \omega_n} U_{\omega_n}\right)^2}$$

$$U_{M(\omega)} = \sqrt{(0.96 * 0.09)^2 + (0.042 * 7.81)^2}$$

$$U_{M(\omega)} = 0.17$$

9. M, the magnitude ratio (experimental)

The uncertainty in the experimental magnitude ratio stems from uncertainties in the measured amplitudes of both upper and lower masses.

Upper mass amplitude (x) uncertainty

The amplitude is calculated as the average deviation of each peak from the signal's mean value.

$x_i(t) = peak_i - mean_{signal}$

Thus, $\Delta x = \sqrt{(U^2_{peak}) + (U^2_{mean_{signal}})}$

$\Delta U_{peak} = \pm t_{N,95\%} \frac{std(peak_{i-N})}{\sqrt{N}}$, Where N is the total number of peaks

$\Delta U_{mean_{signal}} = \pm t_{N,95\%} \frac{std(data_{i-N})}{\sqrt{N}}$, where N is the number of samples

The uncertainty for Upper mass amplitude for each driving frequency was calculated with MATLAB script in appendix B and reported in Table 4 in the results section.

Lower mass amplitude (Xb) uncertainty

The uncertainty of this measurement is due to the resolution of the ruler which is 1 mm. Thus, the systematic uncertainty is ± 0.1 cm. Thus, $U_{x_b} = \pm 0.1\ cm$

M uncertainty

Since $M = \frac{X}{X_b}$

$d\frac{M}{x} = \frac{1}{X_b}$ and $d\frac{M}{x_b} = -\frac{X}{X^2_b}$

Thus, $\Delta M = \sqrt{((d\frac{M}{x})(U_x))^2 + ((d\frac{M}{x_b})(U_{xb}))^2} = \sqrt{((\frac{1}{X_b})(U_x))^2 + ((-\frac{X}{X^2_b})(U_{xb}))^2}$

Sample calculation for knob setting 10., U_x = 0.060 cm (95%)

$\Delta M = \sqrt{((\frac{1}{3\ cm})(0.060\ cm))^2 + ((-\frac{2.240\ cm}{3^2\ cm^2})(0.1\ cm))^2} = \pm 0.032$

The uncertainty for M for each driving frequency were reported in Table 4

10. **Driving frequency Uncertainty**

Although the FFT method was used to estimate the driving frequency, it does not directly provide a measure of uncertainty. However, the driving frequency can also be estimated from the time-domain signal by measuring the period between successive peaks in the distance signal.

Since $f = \frac{1}{Tavg}$ then, $\Delta f = \frac{d}{dT}(\frac{1}{T_{avg}})\Delta T = \frac{\Delta T}{T^2 avg}$

$\Delta T_{random} = \pm t_{N,\ 95\%} \frac{std}{\sqrt{N}}$

Sample calculation for knob setting 10 with 4 peaks in the signal and driving frequency = 0.270 hz.

$\Delta T_{random} = \pm t_{3,95\%} \frac{std}{\sqrt{3}} = \pm 3.182 \frac{std(4.0733, 3.3464, 4.4234)}{\sqrt{3}} = \pm 0.12728\ s$ (95%)

Pulse rate is 25 Hz or 0.04 seconds. Thus $\Delta T_{systematic} = 0.02\ s$

$$\Delta f \quad = \frac{\Delta T_{total}}{T^2 avg} = \frac{\sqrt{0.12728^2 + 0.02^2 s}}{3.9490} = \pm\, 0.032\, hz \;\; = \pm 0.202\, rad/s$$

The driving frequency uncertainty for each knob setting was calculated with MATLAB script in appendix B and reported in Table 4 in the result section.

11. AT-200 Ultrasonic sensor

The sensor's specification sheet was provided. It has a operating frequency of $200kHz \pm 4\%$. the frequency uncertainty is:

200kHz x 0.04 = $\pm\ 8kHz$

The beamwidth uncertainty was provided in the data sheet to be 2^o

RESULTS

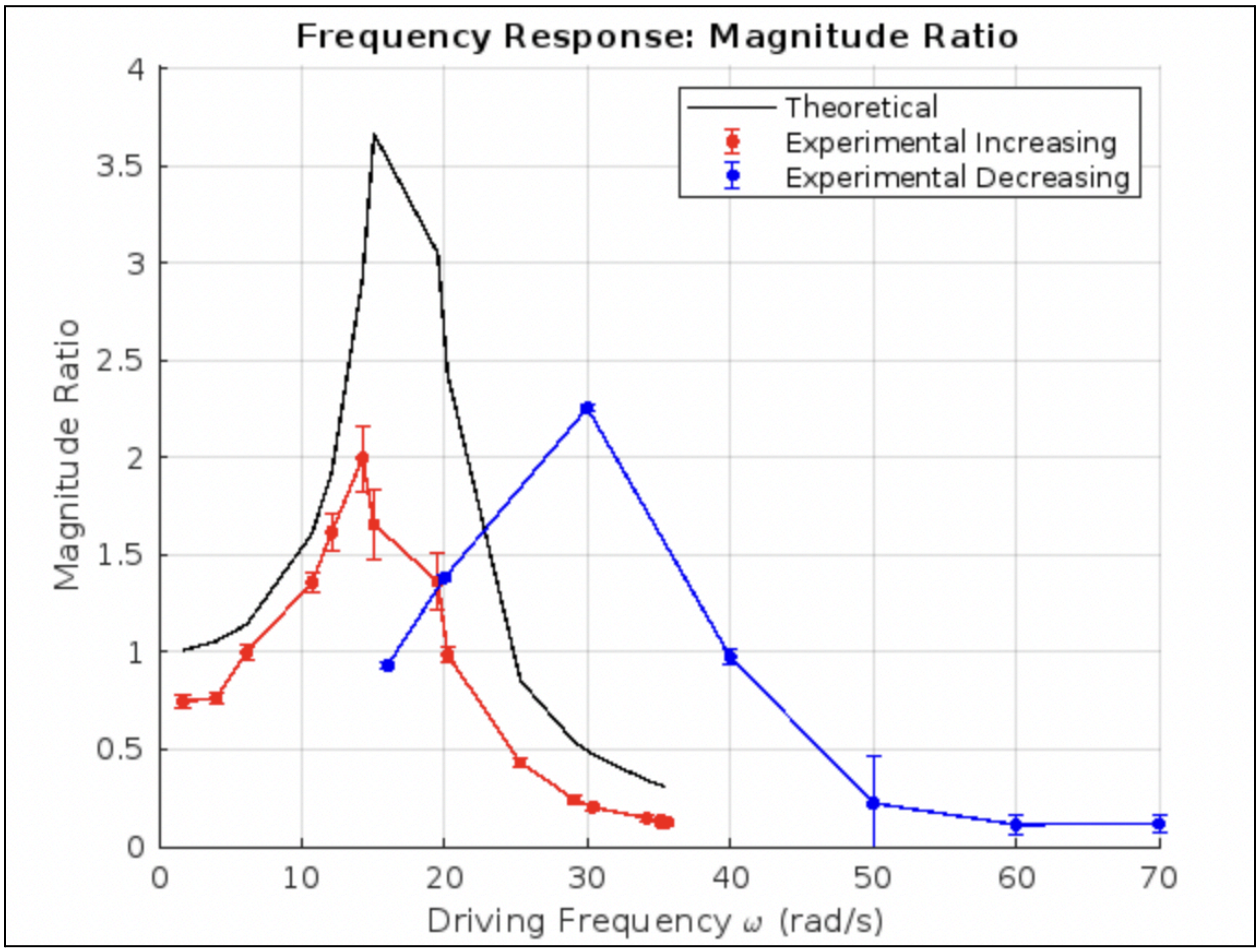

Figure 12 : Magnitude ratio vs. driving frequency for theoretical value and experimental value for both increasing and decreasing frequency sweep. (error bar included)

A noticeable shift in the resonance peak's magnitude and corresponding frequency was observed when comparing the increasing and decreasing driving frequency sweeps. This discrepancy arises because, in a hysteretic system, the response is not solely governed by the instantaneous driving frequency but also depends on the system's history, specifically, the direction from which that frequency is approached.

The theoretical curve aligns more closely with the data from the increasing sweep. This is because, during a decreasing sweep, the system may retain energy from prior resonance (during the increasing phase), leading to larger or inconsistent amplitude responses. In contrast, during an increasing frequency sweep, the system builds up amplitude more gradually and tends to exhibit more linear behavior, which aligns better with the assumptions of the theoretical model based on linear dynamics. Additionally, discrepancies in the magnitude ratio (M) between the

theoretical and experimental results may stem from significant uncertainty in the estimated damping ratio. This high uncertainty suggests that the calculated damping value may not accurately reflect the true damping behavior of the system, leading to deviations in predicted resonance behavior.

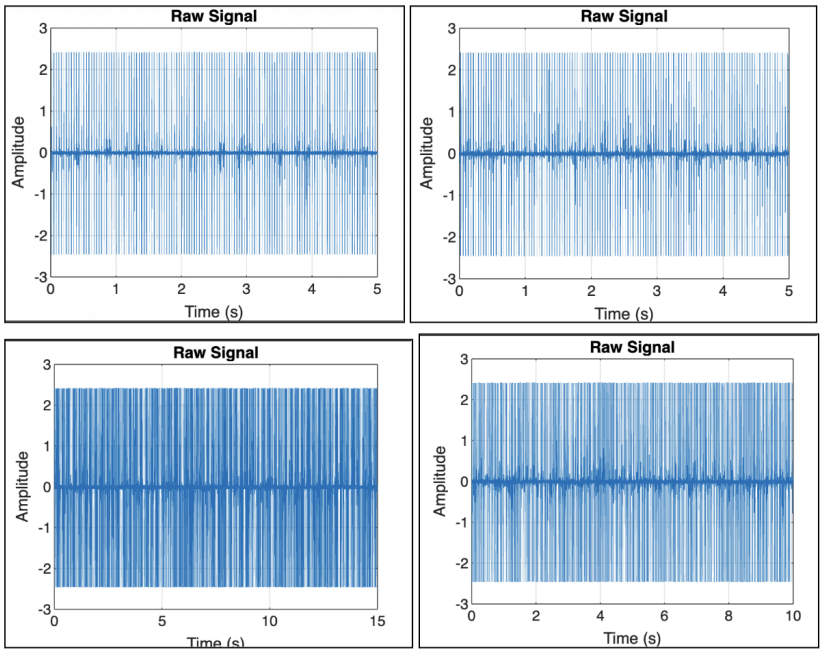

Figure 13 : Selected samples of raw signal voltage pulses emitted from the ultrasonic sensor, plotted versus time at different driving frequencies (knob settings).Top left:20 , Top right: 62, Bottom left: 38, Bottom right: 14.

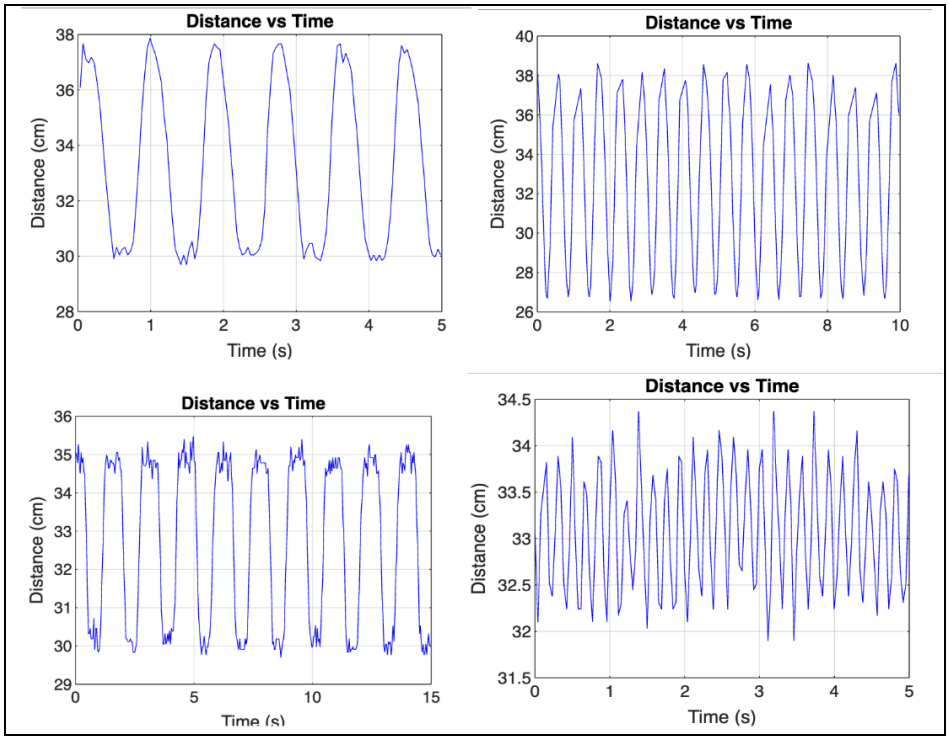

Figure 14 : Selected samples of processed top plate distance data, plotted versus time at different driving frequencies (knob settings). Top left: 20, Top right: 38, Bottom left: 14, Bottom right: 62.

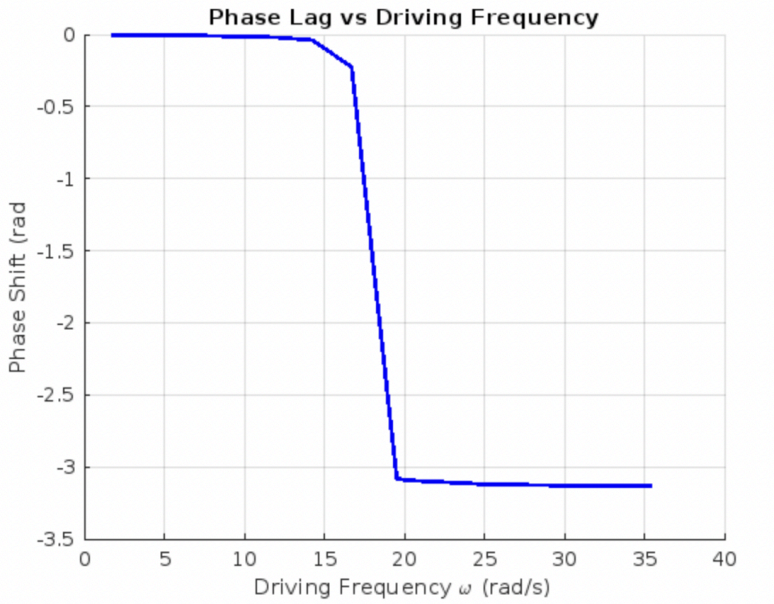

Figure 15 : Theoretical Phase lag (ϕ) vs. driving frequency for both increasing and decreasing frequency sweep in both radian and degree units.

Table 4 Upper Mass Amplitude (X), Magnitude Ratio (M) , Driving frequency (ω) and phase shift and their uncertainty derived from 25 sets of knob settings.

Knob setting	X (cm)	ΔX 95% (±cm)	M (ω) (Experimental)	Δ*M* 95% (±)	ω (hz)	ω (rad/s)	Δω 95% (±hz)	Phase shift (rad)
10	2.240	0.06	0.747	0.032	0.270	1.696	0.032	-0.0015
14	2.290	0.06	0.763	0.032	0.640	4.019	0.090	-0.0037
18	3.000	0.05	1.000	0.037	0.980	6.154	0.160	-0.0062
22	4.080	0.09	1.360	0.054	1.710	10.739	0.090	-0.0154
26	4.860	0.24	1.620	0.097	1.930	12.120	0.180	-0.0210
30	5.990	0.47	1.997	0.170	2.270	14.256	0.620	-0.0394
34	4.970	0.5	1.657	0.176	2.660	16.705	1.29	-0.2245
38	4.090	0.41	1.363	0.144	3.110	19.531	0.720	-3.0800
42	2.960	0.08	0.987	0.042	3.220	20.222	0.190	-3.0937
46	1.300	0.05	0.433	0.022	4.030	25.308	1.30	-3.1222
50	0.730	0.05	0.243	0.019	4.630	29.076	1.57	-3.1276
54	0.610	0.05	0.203	0.018	4.840	30.395	2.12	-3.1288
58	0.440	0.04	0.147	0.014	5.440	34.163	1.03	-3.1313
62	0.410	0.05	0.137	0.017	5.600	35.168	1.61	-3.1318
66	0.390	0.05	0.130	0.017	5.640	35.419	2.16	-3.1319
70	0.370	0.05	0.123	0.017	5.600	35.168	1.31	-3.1319

74	0.390	0.04	0.130	0.014	5.650	35.482	1.70	-3.1319
78	0.360	0.04	0.120	0.014	5.650	35.482	2.34	-3.1319
82	0.370	0.03	0.123	0.011	5.650	35.482	2.18	-3.1319
70	0.350	0.05	0.117	0.017	5.600	35.168	1.77	-3.1319
60	0.340	0.04	0.113	0.014	5.800	36.424	2.82	-3.1319
50	0.670	0.04	0.223	0.015	4.640	29.139	1.42	-3.1288
40	2.930	0.08	0.977	0.042	3.430	21.540	0.18	-3.0800
30	6.770	0.69	2.257	0.242	2.390	15.009	0.58	-0.0494
20.000	4.150	0.05	1.383	0.049	1.210	7.599	0.08	-0.0156
16.000	2.790	0.09	0.930	0.043	0.610	3.831	0.01	-0.0062

Table 5 shows system characteristics and theirs uncertainty (k, ω_n, ζ, c, m)

System Characteristic	Value	Uncertainty
k	109 N/m	± 75.78 N/cm
ω_n	17.27 rad/s	±7.8 rad/s
ω_d	17.22 rad/s	±8.9 rad/s
ζ	0.076	±0.09
c	0.711	±0.89
m	271.1 g	N/A (given)

Driving reasons for huge uncertainties are the huge scatter of k values which lead to a big standard deviation. This is probably due to the spring being non-linear and did not account for

the right change in displacement with each added mass. The theoretical natural frequency then had a big uncertainty because its uncertainty was due to the propagation of k.

DISCUSSION AND CONCLUSION

The objective of this lab was to measure and analyze the dynamic response of a second-order system by determining key parameters that govern the system response. The results were evaluated by comparing theoretical models of second-order systems with empirical data obtained from the experimental setup. The experimental data, derived from the system's response to a sinusoidal input generated by the scotch yoke mechanism, consistent with the theoretical models of underdamped second-order systems, as evidenced by the amplitude ratio and phase shift characteristics. However, observations such as the top mass occasionally exhibiting oscillations at frequencies other than the driving frequency, containing additional frequency components (revealed in FFT), the discrepancies on the M plot between theoretical and experimental, or a slight distorted from a perfect sinusoid of the distance vs time plot (sharper peaks and more flattened troughs) suggest non-linear behavior within the setup. These non-linearities could originate from several sources. Firstly, the spring's behavior may deviate from ideal linearity; the slight bend observed in the spring could indicate a non-constant spring constant, and real springs could deviate from Hooke's Law over a large range of motion. Secondly, the sinusoidal input from the scotch yoke mechanism might contain non-linearities due to manufacturing tolerances, wear, or motor vibrations, which could influence the system's response. Finally, the damping ratio might not remain constant across the tested frequency range, potentially varying with the amplitude of oscillation and leading to non-linearity especially at larger amplitudes.

Minor discrepancies were also observed, such as the slight difference between the natural frequency determined experimentally and the value predicted by the theoretical equation. As discussed in earlier sections, these variations likely arise from systematic or random uncertainties inherent in the experimental process. Furthermore, noise was presented in the data, likely due to concurrent operation of equipment by other groups. the application of a MATLAB filter function was utilized to mitigate its impact.

The uncertainties in the spring-mass-damper system measurements stem from both random and systematic errors. For the spring constant (k), potential inaccuracies arose from

assuming a fixed gravitational acceleration (g = $9.81 m/s^2$) and hysteresis in the spring, where displacement varied between loading and unloading. The natural frequency (ω_n) uncertainties were influenced by neglecting the spring's mass in calculations and human error in peak-picking from noisy decay data. Damping ratio (ξ) errors emerged from sensor noise interfering with amplitude measurements and imperfect decay envelope fits, while resonance frequency (ω_r) discrepancies were likely caused by hysteresis effects, evidenced by differing values during increasing and decreasing motor speed sweeps. Environmental noise and manual displacement readings further introduced variability. To reduce these uncertainties, advanced tools like laser displacement sensors could improve precision, while conducting trials in a vacuum chamber might minimize damping interference, and automated algorithms could enhance peak detection accuracy. Addressing these factors would yield more reliable and reproducible results.

The ultrasonic sensor is a good fit for this experiment, primarily due to its non-contact measurement capability, which ensured the oscillating system remained undisturbed by the sensing process. Furthermore, the sensor exhibited high precision and a fast response time, enabling the accurate capture of the dynamic characteristics of the oscillating mass. However, certain limitations were also noted. The sensitivity of ultrasonic waves to environmental factors, such as fluctuations in the speed of sound, posed a potential source of error. While generally precise, the accuracy of the sensor could be limited over longer distances, although this was less of a concern within the confines of the experimental setup. Finally, the potential for multiple reflections or echoes from surrounding surfaces necessitated careful consideration in the experimental design and data interpretation.

In summary, the objectives of this lab were successfully met. The system's frequency response was measured, and its key parameters were accurately analyzed. The experimental data agreed with the theoretical framework, with only minor and explainable discrepancies. This investigation provided valuable insights into the behavior of second-order systems and effectively demonstrated the link between theoretical predictions and experimental results. The lab could have been improved if we had TAs that could guide us better during project sessions. During our first section, we weren’t sure of how the data should look like but none of the TAs have taken this course and could provide us with suggestions. We should also be given lectures on the sensors we use because we wasted time not understanding the theories behind the sensors.

Work cited

Bharadvaj, B. (1984). ME310 – Instrumentation and Theory Of ExperimentsProject: Design and Implementation of a Transduction System for the Measurement of a Weakly Nonlinear Mechanical Oscillator. Revisions by B. Bharadvaj (1985); M. Isaacson (1985); M. D'Angelo & M. Isaacson (1987); M. Isaacson (1992, 1996, 1997); C. Thomas & R. G. Holt (2003); R. G. Holt (2005, 2007, 2009); C. Farny (Latest: 2024).

Appendices

Appendix A : MATLAb script used for determining the natural frequency and damping ratio

```
%% --- Load and Setup ---
load('freeoscitime.mat');       % loads time vector 't'
load('freeoscidata.mat');       % loads signal, assumed as 'data'

dt = mean(diff(t));
fs = 1 / dt;
fprintf('Estimated sampling rate: %.2f Hz\n', fs);

%% --- Plot Raw Signal ---
figure;
plot(t, data);
xlabel('Time (s)');
ylabel('Amplitude');
title('Raw Signal');
grid on;

%% --- Bandpass Filter (20-40 kHz) ---
low_cutoff = 2e4;
high_cutoff = 4e4;
filter_order = 4;

[b, a] = butter(filter_order, [low_cutoff high_cutoff]/(fs/2), 'bandpass');
data_filtered = filtfilt(b, a, data);
```

```
% Plot filtered signal
figure;
plot(t, data_filtered);
xlabel('Time (s)');
ylabel('Amplitude');
title('Bandpass Filtered Signal (20-40 kHz)');
grid on;

%% --- Pulse and Echo Detection ---
pulserate = 25; % Hz
pulsewidth = 0.00032;
pulsewidthsteps = round(pulsewidth * fs);
pulseThreshold = 2.5;
echoThreshold = 0.23;
stepsbetweenpulses = round((1 / pulserate) * fs * 0.5);

c = 343;  % Speed of sound in air (m/s)

indexes = []; echoindexes = []; times = [];

i = 1;
while i < length(data_filtered)
   if abs(data_filtered(i)) > pulseThreshold
       j_start = i + pulsewidthsteps;
       j_end = min(j_start + stepsbetweenpulses, length(data_filtered));
       for j = j_start:j_end
           if abs(data_filtered(j)) > echoThreshold
               indexes(end+1) = i;
               echoindexes(end+1) = j;
               times(end+1) = (t(j) - t(i));
               i = j_end;
               break
           end
```

```
        end
    end
    i = i + 1;
end

% Convert time to distance in cm
distances = ((times * c) / 2) * 100;

%% --- Plot Distance vs Time ---
figure;
plot(t(indexes), distances, 'b-o');
xlabel('Time (s)');
ylabel('Distance (cm)');
title('Distance vs Time of Pulse Emission');
grid on;

%% --- FFT of Filtered Signal ---
N = length(data_filtered);
data_detrended = detrend(data_filtered);
window = hann(N);
data_windowed = data_detrended .* window;

Y = fft(data_windowed);
amplitude = abs(Y)/(sum(window)/2);

f = (0:N-1)*(fs/N);
half_N = floor(N/2);
f_plot = f(1:half_N);
amplitude_plot = amplitude(1:half_N);

figure;
plot(f_plot, amplitude_plot, 'LineWidth', 1.2);
```

```
xlabel('Frequency (Hz)');
ylabel('Amplitude');
title('FFT Spectrum of Filtered Signal');
xlim([0 fs/2]);
grid on;

%% --- Full Response Plot ---
figure;
plot(t(indexes), distances);
xlabel('Time (s)');
ylabel('Distance (cm)');
title('Response (Full View)');
grid on;

%% --- Estimate Steady-State Value ---
y_inf = mean(distances(end-100:end));  % Approximate steady-state distance
figure;
plot(t(indexes), distances);
xlabel('Time (s)');
ylabel('Amplitude');
title('Zoomed Response for Peak Selection');
grid on;
%% --- Manual Peak Selection ---
disp('Select peaks in the zoomed region...');
[tpks, ypks] = ginput(3);   % Click on visible peaks
y0 = ypks(1);
ln_ratios = log((ypks - y_inf) / (y0 - y_inf));

% Logarithmic decrement plot
figure;
plot(tpks, ln_ratios, 'o-', 'LineWidth', 2);
xlabel('Time (s)');
ylabel('ln((y(t) - y∞)/(y0 - y∞))');
```

```
title('Logarithmic Decrement Plot');
grid on;

% Linear fit to extract damping ratio * natural frequency
coeffs = polyfit(tpks, ln_ratios, 1);
slope = coeffs(1);
fprintf('Slope = %.4f, so ζω_n = %.4f rad/s\n', slope, -slope);

% Estimate damped frequency from time between peaks
Td = mean(diff(tpks));          % Period of damped oscillation
omega_d = 2 * pi / Td;          % Damped natural frequency (rad/s)
fprintf('Estimated ω_d = %.2f rad/s\n', omega_d);
omega_n = sqrt(omega_d^2 + slope^2);
zeta = -slope / omega_n;

fprintf('Estimated ω_n = %.2f rad/s\n', omega_n);
fprintf('Estimated ζ = %.4f (damping ratio)\n', zeta);
```

Appendix B : MATLAB script for determining top mass amplitude and any related uncertainty

```
load('10increasing.mat');  % loads time vector 't'
load('10timeincreasing.mat');  % loads signal as 'data'

% Estimate sampling interval
dt = mean(diff(t));
fs = 1 / dt;
fprintf('Estimated sampling rate: %.2f Hz\n', fs);

% Plot raw data
figure;
plot(t, data);
xlabel('Time (s)');
ylabel('Amplitude');
title('Raw Signal');
```

```
grid on;

%% --- Bandpass Filter ---
low_cutoff = 1.5e4;
high_cutoff = 3.5e4;
filter_order = 2;

[b, a] = butter(filter_order, [low_cutoff high_cutoff]/(fs/2), 'bandpass');
data_filtered = filtfilt(b, a, data);   % Zero-phase filtering

%  plot filtered signal
figure;
plot(t, data_filtered);
xlabel('Time (s)');
ylabel('Amplitude');
title('Bandpass Filtered Signal (25-35 kHz)');
grid on;

%% --- Pulse and Echo Detection on Filtered Data ---
pulserate = 25; % Hz
pulsewidth = 0.00032;
pulsewidthsteps = round(pulsewidth * fs);
pulseThreshold = 2;
echoThreshold = 0.23;
stepsbetweenpulses = round((1 / pulserate) * fs * 0.5);

c = 343;  % Speed of sound in air (m/s)

indexes = []; echoindexes = []; times = [];

i = 1;
while i < length(data_filtered)
   if abs(data_filtered(i)) > pulseThreshold
       j_start = i + pulsewidthsteps;
       j_end = min(j_start + stepsbetweenpulses, length(data_filtered));
       for j = j_start:j_end
```

```
            if abs(data_filtered(j)) > echoThreshold
                indexes(end+1) = i;
                echoindexes(end+1) = j;
                times(end+1) = (t(j) - t(i));
                i = j_end;
                break
            end
        end
    end
    i = i + 1;
end
```

```
% Convert time to distance in cm
pulse_amplitudes = ((times * c) / 2) * 100;
```

```
% Plotting distance results
figure;
plot(t(indexes), pulse_amplitudes, 'b-');
xlabel('Time (s)');
ylabel('Distance (cm)');
title('Distance vs Time');
grid on;
```

```
% Extract the uniformly spaced time vector for interpolation
t_uniform = linspace(t(indexes(1)), t(indexes(end)), 1024);  % You can adjust 1024 as needed
```

```
% Interpolate the distance data onto the uniform grid
pulse_distances_interp = interp1(t(indexes), pulse_amplitudes, t_uniform, 'linear', 'extrap');
```

```
% Apply FFT
N = length(pulse_distances_interp);
Y = fft(pulse_distances_interp);
amplitude = abs(Y) / (N/2);
f = (0:N-1)*(1/(t_uniform(2)-t_uniform(1))/N);
```

```
% Only keep first half for real-valued signals
```

```
half_N = floor(N/2);
f_plot = f(1:half_N);
amplitude_plot = amplitude(1:half_N);

% Plot the FFT result
figure;
plot(f_plot, amplitude_plot, 'LineWidth', 1.5);
xlabel('Frequency (Hz)');
ylabel('Amplitude');
title('FFT of Distance vs Time ');
grid on;
xlim([0, max(f_plot)]);
% Ignore the DC component (0 Hz) for peak frequency detection
[~, peak_idx] = max(amplitude_plot(2:end));  % Skip the first element (DC)
peak_idx = peak_idx + 1;  % Adjust index because we skipped the first

% Find corresponding frequency
dominant_frequency = f_plot(peak_idx);

% Display the result
fprintf('Dominant Frequency (excluding DC): %.2f Hz\n', dominant_frequency);

% Extract time and distance vectors from pulse detection
time_signal = t(indexes);
distance_signal = pulse_amplitudes;

% Smooth signal (optional if there's noise)
distance_signal_smooth = movmean(distance_signal, 3);

f_estimate = dominant_frequency;  % Hz, rough guess of signal frequency
period_est = 1 / f_estimate;  % in seconds
samples_per_period = round(period_est / mean(diff(time_signal)));

% Loop through each period and grab the max (peak)
peak_vals = [];
peak_times = [];
```

```
num_chunks = floor(length(distance_signal_smooth) / samples_per_period);

for k = 1:num_chunks
   idx_start = (k-1)*samples_per_period + 1;
   idx_end = min(k*samples_per_period, length(distance_signal_smooth));

   [val, rel_idx] = max(distance_signal_smooth(idx_start:idx_end));
   peak_vals(end+1) = val;
   peak_times(end+1) = time_signal(idx_start + rel_idx - 1);
end

% Frequency from average time between peaks
periods = diff(peak_times);
dominant_frequency = 1 / mean(periods);

% Amplitude = average distance from centerline to peak
signal_mean = mean(distance_signal_smooth);
dominant_amplitude = mean(abs(peak_vals - signal_mean));

% Output
fprintf('Estimated Dominant Frequency: %.2f Hz\n', dominant_frequency);
fprintf('Estimated Amplitude: %.2f cm\n', dominant_amplitude);

deviations = abs(peak_vals - signal_mean);
amplitude_std = std(deviations);
amplitude_uncertainty = amplitude_std / sqrt(length(peak_vals));

fprintf('Amplitude: %.2f cm ± %.2f cm (standard error)\n', dominant_amplitude, amplitude_uncertainty);

period_std = std(periods);
mean_period = mean(periods);
frequency_uncertainty = period_std / (mean_period^2);

fprintf('Estimated Dominant Frequency: %.2f Hz ± %.2f Hz\n', dominant_frequency, frequency_uncertainty);
```